

Optically controlled noise and small-signal behaviour of READ avalanche diode

G N Dash¹, J K Mishra*, I P Mishra and S R Pattanaik

P G Department of Physics, Sambalpur University, Jyoti Vihar, Sambalpur-768 019, Orissa, India

*P G Department of Physics, G M College (Autonomous), Sambalpur-768 004, Orissa, India

E-mail : gndash@rediffmail.com

Received 10 August 2001, accepted 25 February 2003

Abstract : A new analytical model to study the effect of optical radiation on the noise behaviour of a Read type IMPATT diode is presented. The application of this method to a Si-Read diode reveals some interesting features of reduction in the resonance like noise peak due to optical injection.

Keywords : IMPATT, optical, radiation, noise.

PACS Nos. : 85/ kk, 73.40, -c

IMPATT (IM Pact Avalanche Transit Time) diodes constitute a major source of microwave power. The impact ionisation process responsible for power generation in an IMPATT diode is also responsible for the generation of avalanche noise in the diode. With the modernisation of device technology, realisation of low noise in semiconductor devices has become an important aspect for research [1,2]. In recent years, optical control of microwave properties in IMPATT diodes has gained revived interest. A good numbers of work on optical control of IMPATT diodes like optical switching [3,4], tuning [5,6] and injection locking [7,8] have been reported. In addition, optical carrier injections leading to an improvement in oscillator noise have also been demonstrated [9,10]. More recently, Herbert and Davis [11] have suggested tunneling and/or optical injection as a means of reducing noise in IMPATT diode. The former (tunnel injection) has already been considered by us [12] with interesting results. We now consider the optical injection in this paper for possible means of achieving low noise in IMPATT diode. We have confined our discussion on the small signal regime and the Read model because both of these permit analytical solutions; analytical solutions although consid-

ered qualitative in nature, are highly instructive and clearly show directions for improvements. Using our analytical model, we have studied the noise behaviour of a Si Read diode at different level of optical radiation. Our results show some interesting features of increase in the level of optical radiation on the noise behaviour of Read type IMPATT diodes.

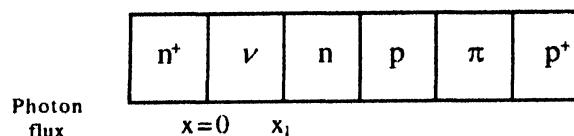


Figure 1. Schematic diagram of the double Read IMPATT diode showing the doping pattern of different layers.

A generalised Read diode model is considered which can be used to investigate the properties of not only the n-type (n^+vnp^+) and p-type ($n^+p\pi p^+$) Read diodes but also the properties of double Read ($n^+vnp\pi p^+$) diode in presence of optical radiation as shown in Figure 1. The steady state carrier continuity equation in presence of optical radiation can be written as [for definition please refer to the list of symbols]

¹ Corresponding Author

$$\begin{aligned} \frac{dJ_p(x)}{dx} &= \alpha_n J_n(x) + \alpha_p J_p(x) + qG_{op}(x) \\ &= \alpha_n J - \alpha_n J_p(x) + \alpha_p J_p(x) + qG_{op}(x). \end{aligned} \quad (1)$$

The optical generation rate G_{op} may be expressed as [13]

$$G_{op}(x) = \frac{P_{opt}(1-R)\alpha_a}{Ah\nu} e^{-\alpha_a x} = \phi_N \alpha_a e^{-\alpha_a x}, \quad (2)$$

where $\phi_N = \frac{P_{opt}(1-R)}{Ah\nu}$ is the number of photons striking per unit area per unit time. Eq. (1) is solved to obtain an expression for total current density $J = J_n + J_p$, in presence of optical radiation, with the boundary conditions

$$J_p = J'_{ps}, \quad J_n = J - J'_{ps} \text{ at } x = x_1 \quad (3a)$$

$$\text{and } J_n = J'_{ns}, \quad J_p = J - J'_{ns} \text{ at } x = x_2, \quad (3b)$$

$$\text{where } J'_{ps} = J_{ps} + q\phi_N(1 - e^{-\alpha_n x_1}) \quad (4a)$$

$$\text{and } J'_{ns} = J_{ns} + q\phi_N(e^{-\alpha_n x_2} - e^{-\alpha_n w}). \quad (4b)$$

J_{ps} and J_{ns} are the reverse hole and electron saturation current densities at the respective boundaries. Rearranging eq. (1), multiplying with the integrating factor $e^{(\alpha_n - \alpha_p)x}$ and integrating between the limits x_1 and x_2 with appropriate boundary conditions mentioned above, we get

$$\begin{aligned} (J - J'_{ns})e^{(\alpha_n - \alpha_p)x_2} - J'_{ps}e^{(\alpha_n - \alpha_p)x_1} \\ = \frac{\alpha_n J [e^{(\alpha_n - \alpha_p)x_2} - e^{(\alpha_n - \alpha_p)x_1}]}{\alpha_n - \alpha_p} \\ + \frac{q\phi_N \alpha_a [e^{(\alpha_n - \alpha_p - \alpha_a)x_2} - e^{(\alpha_n - \alpha_p - \alpha_a)x_1}]}{\alpha_n - \alpha_p - \alpha_a}. \end{aligned} \quad (5)$$

Dividing both sides of eq. (5) by $e^{(\alpha_n - \alpha_p)x_1}$ and putting

$x_2 - x_1 = x_g$ the avalanche region width, we have

$$\begin{aligned} (J - J'_{ns})e^{(\alpha_n - \alpha_p)x_g} - J'_{ps} = \frac{\alpha_n J [e^{(\alpha_n - \alpha_p)x_g} - 1]}{\alpha_n - \alpha_p} \\ + \frac{q\phi_N \alpha_a e^{-\alpha_a x_1} [e^{(\alpha_n - \alpha_p - \alpha_a)x_g} - 1]}{\alpha_n - \alpha_p - \alpha_a} \end{aligned} \quad (6)$$

Rewriting eq. (6) and keeping in mind that

$$J'_s = J'_{ns} + J'_{ps} \text{ we get}$$

$$\begin{aligned} J[\alpha_n - \alpha_p e^{(\alpha_n - \alpha_p)x_g}] = J'_s(\alpha_n - \alpha_p e^{(\alpha_n - \alpha_p)x_g}) \\ + (\alpha_n J'_{ns} + \alpha_p J'_{ps})[e^{(\alpha_n - \alpha_p)x_g} - 1] \end{aligned}$$

$$\begin{aligned} \phi_N \alpha_a (\alpha_n - \alpha_p) e^{-\alpha_a x_1} [e^{(\alpha_n - \alpha_p - \alpha_a)x_g} - 1] \\ \alpha_n - \alpha_p - \alpha_a \end{aligned}$$

The total current density J , follows directly from eq. (7) as

$$\begin{aligned} J = J'_s + (\alpha_n J'_{ns} + \alpha_p J'_{ps}) \left| \frac{e^{(\alpha_n - \alpha_p)x_g} - 1}{\alpha_n - \alpha_p e^{(\alpha_n - \alpha_p)x_g}} \right. \\ \left. \left[\frac{q\phi_N \alpha_a (\alpha_n - \alpha_p) e^{-\alpha_a x_1}}{\alpha_n - \alpha_p - \alpha_a} \frac{e^{(\alpha_n - \alpha_p - \alpha_a)x_g} - 1}{e^{(\alpha_n - \alpha_p)x_g}} \right] \right. \end{aligned} \quad (8)$$

This expression for J in the absence of optical illumination, is the same as that of Elta and Haddad [14] in the absence of tunneling. This value of current density in presence of optical radiation is used to estimate an effective ionisation rate α_{eff} (equal for both electrons and holes), which takes into account the actual values of experimentally determined ionisation rates used in the above analysis. α_{eff} may be defined as that value of ionisation rate, which will generate the same J in the generation region as by the actual experimentally determined values of ionisation rates. An expression for α_{eff} may be obtained in the following way.

For the case of $\alpha_n = \alpha_p = \alpha_{eff}$, the steady state continuity equation may be written as

$$\frac{dJ_p(x)}{dx} = \alpha_{eff} J + qG_{op}(x). \quad (9)$$

Integrating this between the limits x_1 and x_2 with appropriate boundary conditions and rearranging, the effective ionisation rate may be expressed as

$$\alpha_{eff} = \frac{J - J'_s - q\phi_N e^{-\alpha_a x_1} (1 - e^{-\alpha_a x_g})}{J x_g}. \quad (10)$$

This value of effective ionisation rate is used to solve the Read equation to obtain the expressions for the device properties. Thus, the use of α_{eff} removes the error arising out of the assumption of equal ionisation rates for electrons and holes in Read equation.

For the noise analysis the noise current density is considered to have three components namely J_{no} , due to critical electric field necessary to maintain a steady avalanche, J_{nc} , due to AC field caused by J_{no} and a displacement noise current density J_d . An expression for J_{no} is obtained following the method of Hines [15] as

$$J_{no} = \left| \frac{2qJB}{\omega^2 \tau_x^2 A} \right|^{1/2} \quad (11)$$

The expression for J_{ne} and displacement current density J_d are obtained by solving Read equation under optical illumination following our method described in [12] as

$$J_{ne} = \frac{2x_g E_{gn} \alpha'_{eff} J}{i\omega\tau_g + 2(1 - \alpha'_{eff} x_g)} \quad (12)$$

$$\text{and } J_d = i\omega E_{gn}. \quad (13)$$

where $\tau_g = x_g / v_d$ and the expression for the amplitude of AC noise field in the generation region E_{gn} , is the same as in [12]. Now, following a similar procedure as in [12], the mean square noise voltage per bandwidth can be obtained as

$$\frac{\langle v_n^2 \rangle}{B} = \frac{2qJ}{\omega^2 \tau_g^2 A} \left[1 + \frac{x_d \sin \theta_d}{x_g \theta_d} - \frac{ix_d(1 - \cos \theta_d)}{x_g \theta_d} \right] \quad (14)$$

The small-signal properties are computed from the diode impedance Z_D by defining the diode admittance $Y_D = 1/Z_D$ from which the diode conductance (G) and the diode resistance Z_R are obtained respectively as the real part of Y_D and Z_D . It may be mentioned here that the diode conductance and diode resistance which shows negative values for a certain range of frequency (defined as bandwidth), are useful parameters to assess the small-signal performance of the diode.

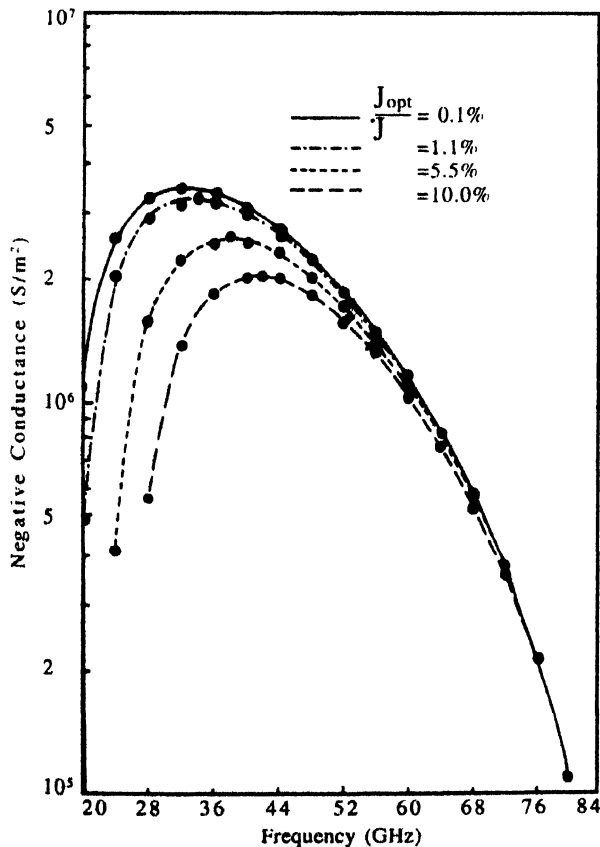


Figure 2. Variation of device negative conductance as a function of frequency for different level of optical injection.

The above analytical method is used to study the noise behaviour of a Si-based $n^+p\pi p^+$ Read diode at different level of optical injections. The total width of the diode is taken as $1 \mu\text{m}$ and the avalanche region width as $0.2 \mu\text{m}$. The reverse saturation electron and hole current densities J_n and J_p are taken as $1 \mu\text{A}/\text{m}^2$ each. The optical absorption peak wavelength and the optical absorption coefficient at this wavelength for Si are taken from [13]; $\lambda = 0.8 \mu\text{m}$ and $\alpha_a = 10^5 \text{m}^{-1}$. The operating current density is chosen to be $J = 5 \times 10^7 \text{A}/\text{m}^2$. The generation region electric field required to generate this value of J , in presence of optical radiation, is determined by an iterative sub-program in the following way. First, a trial value of the electric field is chosen and the total current density J in presence of optical radiation, is computed following eq. (8). If this value differs from the chosen J , then the electric field is suitably varied, over several iterations, until the computed J is equal to the chosen J within an accuracy of 0.05%. The percentage of optical current density J_{opt}/J is then determined. This process is repeated for different ϕ_N values and the mean square noise voltage as well as the small-signal parameters like diode conductance and diode resistance is estimated in each case. The results are presented in Table 1 and Figures 2-4.

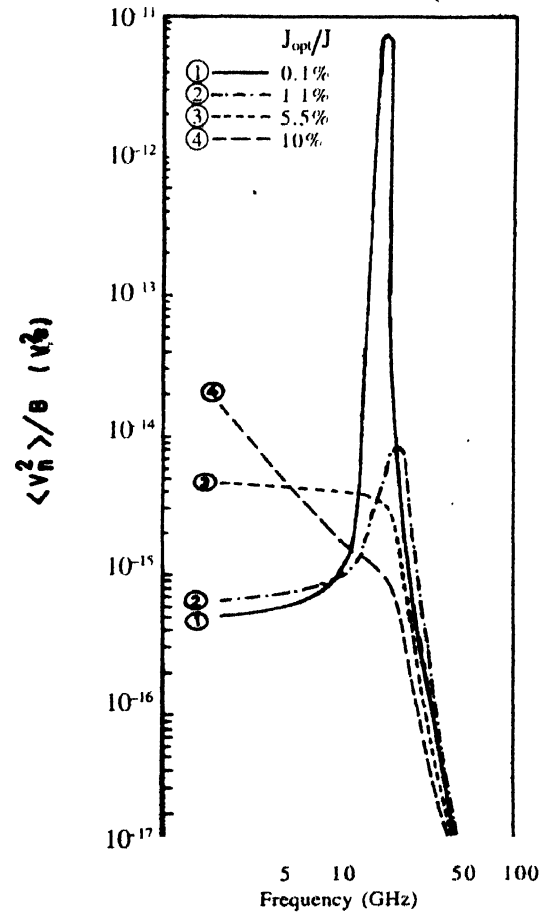


Figure 3. Variation of mean square noise voltage per bandwidth as a function of frequency for different level of optical injection

Figure 2 shows the frequency *versus* conductance plots for the Si-Read diode for different level of optical injection. It can be seen from Table 1 and Figure 2 that the device negative conductance ($-G_p$) at optimum frequency (f_p) decreases steadily with increase in optical injection. Further, it is observed from Figure 2 that the bandwidth of the device decreases considerably as the optical injection level increases. It can also be observed from Table 1 that the device property like negative resistance ($-Z_{Rp}$) and negative conductance ($-G_p$) at optimum frequency, which are indicative of power output from the device, decreases with increase in photon injection. Figure 3

Table 1. Small signal and noise properties of the Si Read IMPATT diode at different level of optical illumination.

J_{opt}/J (%)	$\langle v_n^2 \rangle / B$ ($10^{-14} \text{ V}^2 \text{ s}$)	f_p (GHz)	$-G_p$ (10^6 S/m^2)	$-Z_{Rp}$ ($10^4 \Omega \text{ m}^2$)	$\langle v_n^2 \rangle / B$ at f_p ($10^{-17} \text{ V}^2 \text{ s}$)	NM at f_p
0.11	722	32	3.51	1.26	5.93	1790
1.1	8.06	34	3.31	0.969	3.88	1530
2.2	2.05	34	3.10	0.921	3.87	1330
5.5	0.362	38	2.60	0.547	1.78	1240
10.0	0.181	42	2.09	0.332	0.865	999

shows the plots for variation of the mean square noise voltage as a function of frequency at different level of optical injection. It is observed from this figure that, a sharp peak of $7.22 \times 10^{-12} \text{ V}^2 \text{ s}$ at the resonant frequency is recorded for a very low level of photon injection. However, this noise peak drastically reduces to $8.06 \times 10^{-14} \text{ V}^2 \text{ s}$ when the level of photon injection is nominally increased to 1% (Table 1). It is also observed from Figure 3 and Table 1 that as the level of photon injection increases, the noise peak further decreases and at about 5% of optically generated current the peak completely vanishes. This can be understood by noting that, under ideal condition with negligible reverse saturation current, the generation region behaves like a purely reactive circuit with $R_g \rightarrow 0$ and L_g and C_g in parallel with each other. This gives rise to a sharp peak of Z_g and hence $\langle v_n^2 \rangle / B$ as $\omega \rightarrow \omega_g$. However, due to optical injection the reverse saturation current increases which increases the resistive component (R_g) of the generation region. This increases the third term in the denominator of Z_g [12] which in turn suppresses the peak in $\langle v_n^2 \rangle / B$ curve. It can also be seen from Table 1 that the value of mean square noise voltage at optimum frequency (f_p) shows a steady decrease from $3.88 \times 10^{-17} \text{ V}^2 \text{ s}$ to $0.86 \times 10^{-17} \text{ V}^2 \text{ s}$ with increase in the level of photon injection from 0.1% to 10%. The noise measure defined as the ratio $\langle v_n^2 \rangle > A / 4BkT(-Z_{Rp})$, is considered as an indicator of noise power to useful power ratio. This quantity has been plotted as a function of frequency in Figure 4 for different level of optical radiation. Each of the curves shows a minimum at a frequency, which is approximately twice or more than that of the optimum frequency (f_p). This frequency (noise measure minimum) may be chosen for operation of the diode for very low noise. However, the power output at this frequency would be drastically low. In addition, it is observed that the noise measure minimum constantly increases with increase in the

level of optical radiation. Thus, this frequency corresponding to noise measure minimum is unsuitable for operation if one intends to harness the benefit of optical radiation. On the other hand, at optimum frequency, the noise measure is observed to

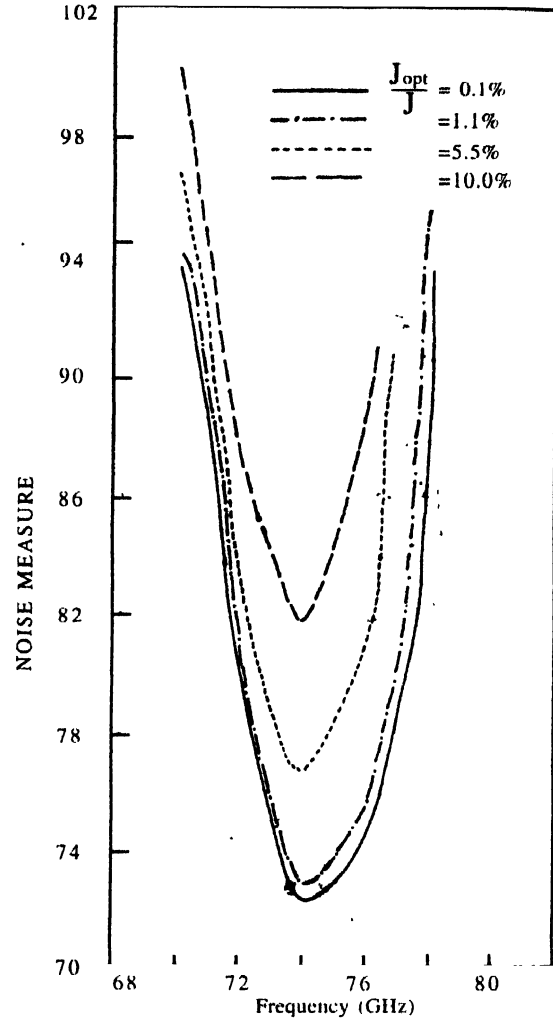


Figure 4. Noise measure as a function of frequency for different level of optical injection.

constantly decrease (Table 1) with increase in level of optical injection. This is partly due to increase in optimum frequency and partly due to decrease in mean square noise voltage with increase in optical radiation. Thus, a suitably tailored dose of photon for operation at the optimum frequency, will not only reduce the noise to a tolerable level but will keep the power output at a moderate level.

An analytical model to study the noise as well as small-signal behaviour of a Read diode in presence of optical radiation is presented in this Note. This method can be applied to any type of Read diode. A Silicon-based IMPATT Read diode is studied with this new model at different level of optical radiation. The results show that it is possible to control the device properties by a suitable level of photon injection such that the mm-wave properties do not degrade appreciably, at the same time the noise reducing to a tolerable level.

Acknowledgment

The authors wish to acknowledge the Department of Science and Technology, Government of India for financial support of this work through a major research project (SP/S2/M-12/98).

References

- [1] G N Dash, J K Mishra and A K Panda *Solid-State Electronics* **39** 1473 (1996)
- [2] J K Mishra, A K Panda and G N Dash *IEEE Trans. Electron Devices* **ED-44** 2143 (1997)
- [3] H W Yen, M K Barnoski, R G Hunsperger and R T Melville *Appl. Phys. Lett.* **31** 120 (1977)
- [4] R A Kiehl *IEEE Trans. Electron Devices* **ED-27** 426 (1980)
- [5] A J Seeds, J F Singleton, S P Brunt and J R Forrest *IEEE J. Light Wave Tech.* **LT-5** 403 (1987)
- [6] C Chiu and J Freyer *Proc. Inst. Elec. Eng.* **131** 28 (1984)
- [7] A J Seeds and J R Forrest *Electron Lett.* **14** 829 (1978)
- [8] H W Yen *Appl. Phys. Lett.* **36** 680 (1980)
- [9] A J Seeds and J R Forrest *Electron Lett.* **17** 865 (1981)
- [10] P M Pitner, R J Gutmann and J M Borrego *Proc. Inst. Elec. Eng.* **128** 149 (1982)
- [11] D C Herbert and R G Davis *IEEE Trans. Electron Devices* **ED-47** 197 (2000)
- [12] G N Dash, J K Mishra and S K Nayak *IEEF Tech. Review* **16** 243 (1999)
- [13] S M Sze *Physics of Semiconductor Devices* (New Delhi: Wiley Eastern), 2nd Edn. (1987)
- [14] M E Elta and G I Haddad *IEEE Trans. Electron Devices* **ED-25** 694 (1978)
- [15] M E Hines *IEEE Trans. Electron Devices* **ED-13** 158 (1966)

Annexure

- A : area of the diode
- B : band width
- C_d : drift region capacitance
- C_g : generation region capacitance
- f_p : optimum frequency
- G_p : diode conductance at f_p
- h : Planck's constant
- $h\nu$: photon energy
- J_n : conduction current density for electrons
- J_{n0} : electron reverse saturation current density
- J_p : conduction current density for holes
- J_{p0} : hole reverse saturation current density
- L_g : generation region inductance
- P_{opt} : average incident optical power
- q : electronic charge
- R : reflection coefficient of the surface
- R_g : generation region resistance
- v_d : saturated drift velocity of carriers
- W : width of the depletion layer
- x : distance in depletion region
- x_d : drift region width
- x_g : generation region width
- Z_d : drift region impedance
- Z_p : diode impedance
- Z_g : generation region impedance
- Z_{Rp} : diode resistance at f_p
- α_o : optical absorption coefficient
- α'_{eff} : field derivative of α_{eff}
- α_n : ionisation rate for electrons
- α_p : ionisation rate for holes
- ν : frequency of light
- ω : angular frequency of AC
- ω_g : generation region angular frequency
- τ_i : time between successive collisions
- ϵ : permittivity of the semiconductor
- θ_d : transit angle for drift region